JOURNAL OF MATERIALS SCIENCE 27 (1992) 3925–3931

Superplastic deformation of Ti–6Al–4V extruded tube

A.WISBEY, P.G.PARTRIDGE, A.W.BOWEN
Materials and Structures Department, Royal Aerospace Establishment, Farnborough, Hampshire GU14 6TD, UK

Superplastic forming using conventional alloys and product forms may be a cost effective route for component manufacture. In this paper superplastic deformation of Ti–6Al–4V extruded tube is examined in terms of the strain anisotropy, microstructural changes, the texture and the post-formed tensile properties. Superplastic deformation with low flow stresses over a wide range of strain rates was observed. Strain anisotropy and surface roughening occurred during deformation and was associated with the two-phase, aligned and banded microstructure. A small reduction in the tensile properties was found and changes in the texture were noted after superplastic deformation.

1. Introduction

Superplastic forming (SPF) has been combined with diffusion bonding (DB) in the manufacture of large sheet SPF/DB aerospace structures to obtain substantial reductions in manufacturing costs and component weight. Recently there has been interest in the use of other product forms (e.g. bars) for the manufacture of components such as helicopter impellers in Ti–6Al–4V [1] and discs in the near β-alloy Ti–9.5V–3Al–2.5Mo [2]. The use of SPF with "off-the-shelf" alloys and product forms could significantly reduce the cost of alloy development and manufacture, and is being investigated in Japan [3]. Minor alloying additions and changes in the thermo-mechanical processing of current commercial alloys of aluminium [3] and titanium [4, 5] may lower the optimum temperature for SPF and reduce the stress and strain anisotropy. Previous work has shown that superplastically deformed Ti–6Al–4V rectangular section bar, with an aligned and banded α/β microstructure, deforms anisotropically [6] and similar behaviour is anticipated in other Ti–6Al–4V product forms with non-ideal SPF microstructures. However, commercially useful superplastic deformation is possible with non-ideal SPF microstructures [7]. In this work the microstructural changes, the SPF parameters, the strain anisotropy and the post-formed tensile properties of Ti–6Al–4V extruded tube are examined and compared with previous work in the literature.

2. Experimental procedure

Extruded Ti–6Al–4V tube of 100 mm outside diameter and 6.5 mm wall thickness (Fig. 1a) was cut in half and pressed flat at ~ 700 °C in vacuum (Fig. 1b). From the resultant plates, elevated temperature and standard room-temperature tensile test pieces were machined in the longitudinal (L) and hoop (transverse T) directions. To prevent deformation around the loading pins during superplastic deformation, 4.5 mm thick Ti–6Al–4V support plates were electron beam welded on to the test pieces. The room-temperature tensile properties were measured on the test pieces deformed at 925 °C; a 47 mm gauge length was machined centrally.

Tests were carried out at a constant temperature of 925 ± 3 °C under a positive pressure of gettered argon in a vertical split-tube three-zone furnace. The test piece elongation was limited to 300% on a 25 mm gauge length. After deformation the test-piece was cooled to 600 °C at 25 °C min^{-1} in the gettered argon atmosphere. The test pieces were pre-strained to 4% elongation at a strain rate of $\dot{\varepsilon} = 3.2 \times 10^{-4}\ s^{-1}$. Within the first 25% elongation the initial true flow stresses, over a range of true strain rates ($\dot{\varepsilon} = 2 \times 10^{-5}$–$6 \times 10^{-4}\ s^{-1}$) were determined by cross-head velocity, V, stepping. The strain-rate sensitivity index, m, was obtained using the equation for stress, σ, versus strain rate, $\dot{\varepsilon}$, under conditions of no strain hardening

$$\sigma = K\dot{\varepsilon}^m \quad (1)$$

Whence

$$m = \frac{\ln(P_1/P_2)}{\ln(V_1/V_2)} \quad (2)$$

where P is the load at crosshead velocity, V. Then the test pieces were deformed at nominally constant strain rate by increasing V every 25% elongation up to 300% elongation, to give strain rates of $\dot{\varepsilon}_1 = 5 \times 10^{-5}\ s^{-1}$, $\dot{\varepsilon}_2 = 3.2 \times 10^{-4}\ s^{-1}$, $\dot{\varepsilon}_3 = 1 \times 10^{-3}\ s^{-1}$ and $\dot{\varepsilon}_4 = 1 \times 10^{-2}\ s^{-1}$. The load was continuously monitored and the flow stress calculated. The true area strain and the plastic strain ratio ($R = \ln(w/w_o)/\ln(t/t_o)$, where w, w_o, t, t_o are the final and initial width and thicknesses, respectively) were measured after testing at 925 °C.

Microstructural changes in the Ti–6Al–4V were evaluated metallographically; the α/β phase proportions, the mean linear intercept length of α-phase in the L, T and ST directions and the α-phase aspect ratio were determined. Texture analysis is reported elsewhere [8] on the as-received material after pressing and following superplastic deformation in the L and T directions. Surface roughness, R_a, values (R_a = arithmetic mean of the profile from the mean line) for a traverse length of 17.5 mm along the tensile axis of superplastically deformed L and T test pieces were obtained. Room-temperature tensile tests to BS.18 ($\dot{\varepsilon} = 3 \times 10^{-4}\ s^{-1}$ to 0.5% strain, then $10^{-3}\ s^{-1}$) were performed. Material was tested in the as-pressed condition, after SPF thermal cycling (0% deformation, 7.5 h at 925 °C ≡ deformation at $\dot{\varepsilon}_1$) and as-superplastically deformed at $\dot{\varepsilon}_1$.

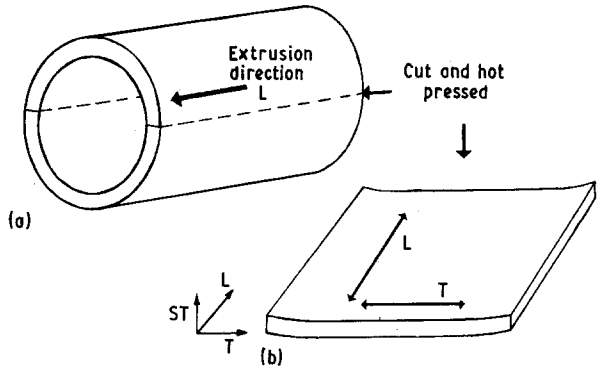

Figure 1 Extruded tube: (a) as-received, (b) after cutting and pressing flat.

3. Results

3.1. SPF parameters

In the present tests uniform superplastic deformation was obtained up to the maximum elongation of 300 % (true strain 1.38) at $\dot{\varepsilon}_1$ for both L and T test pieces (Fig. 2). Even at $\dot{\varepsilon}_3 = 1 \times 10^{-3}\ s^{-1}$ there was little local necking (Fig. 2). At the highest strain rate ($\dot{\varepsilon}_4 = 1 \times 10^{-2}\ s^{-1}$) significant local necking was observed after 160 % elongation.

The initial true flow stresses increase approximately logarithmically with strain rate in the range of strain rates tested at 925 °C (Fig. 3). The flow stresses were greater in the L-oriented test pieces. The *m*-values are plotted in Fig. 4; the loads at low strain rates ($\dot{\varepsilon} < 8 \times 10^{-5}\ s^{-1}$) were small and difficult to measure consistently, which resulted in a scatter band of $m = 0.55$–0.84. Almost constant *m*-values were observed for $\dot{\varepsilon} > 8 \times 10^{-5}\ s^{-1}$, where $m \sim 0.55$ for L test pieces and ~ 0.66 for T test pieces.

At a strain rate of $\dot{\varepsilon}_1$ the flow stress was significantly lower than the other strain rates ($\dot{\varepsilon}_2$ and $\dot{\varepsilon}_3$, Fig. 5). The true flow stresses of the T and L test pieces were similar at these strain rates. At $\dot{\varepsilon}_3 = 1 \times 10^{-3}\ s^{-1}$ similar initial flow stresses to tests at $\dot{\varepsilon}_2$ were measured;

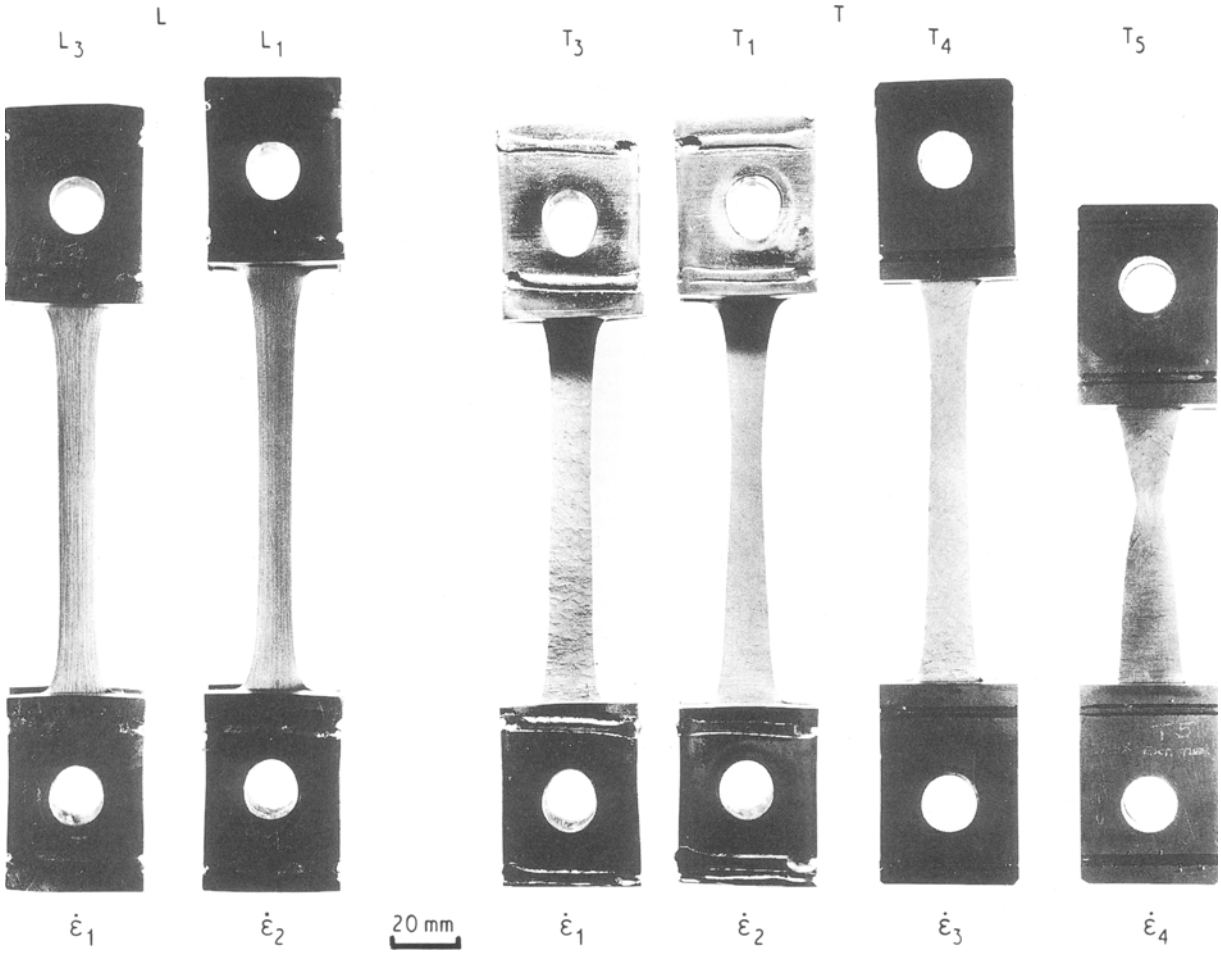

Figure 2 Extruded tube test-pieces after deformation at 925 °C, $\dot{\varepsilon}_1 = 5 \times 10^{-5}\ s^{-1}$, $\dot{\varepsilon}_2 = 3.2 \times 10^{-4}\ s^{-1}$, $\dot{\varepsilon}_3 = 1 \times 10^{-3}\ s^{-1}$, $\dot{\varepsilon}_4 = 1 \times 10^{-2}\ s^{-1}$. L – longitudinal, T – transverse.

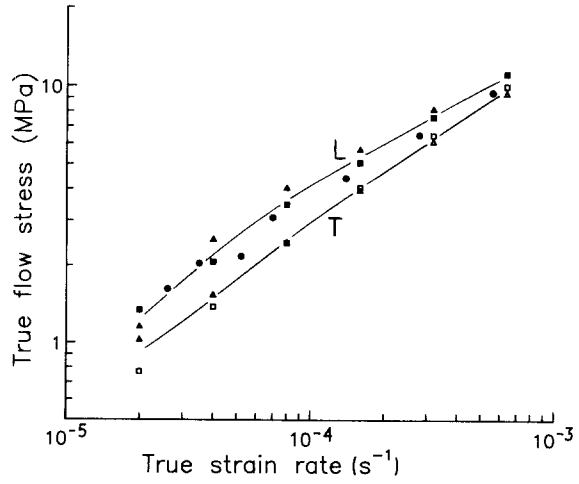

Figure 3 Initial true flow stress versus true strain rate determined by the stepped strain-rate technique for L and T test pieces: (●) L_1, (▲) L_2, (■) L_3, (△) T_2, (□) T_3.

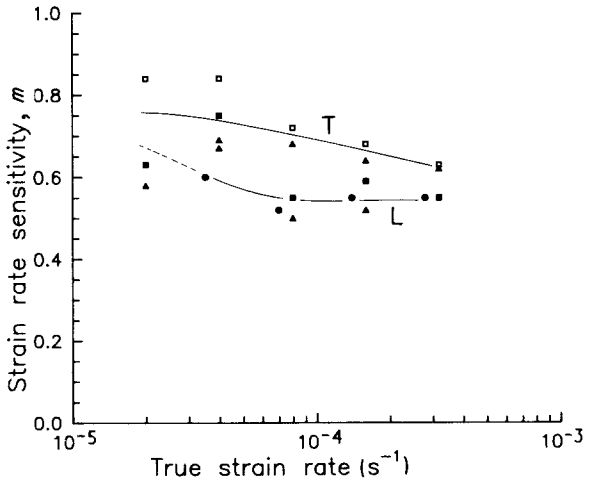

Figure 4 Initial strain rate sensitivity index, m, versus true strain rate determined by the stepped strain-rate technique at 925 °C. Test pieces: (●) L_1, (▲) L_2, (■) L_3, (△) T_2, (□) T_3.

however, the flow stress at $\dot{\varepsilon}_3$ increased more rapidly with strain than at $\dot{\varepsilon}_2$.

The plastic deformation at elevated temperature was anisotropic; R-values less than 1.0 (Fig. 6) were achieved for all test pieces indicating greater strain through the thickness than in the width. The R-value increased with increasing strain. The low values at H in Fig. 6 were obtained near the test piece head and were caused by the constraints imposed by the test piece head on plastic flow in the gauge length. The curves tended towards a maximum of 0.65 and 0.80 for T and L test pieces, respectively; the exact R versus ε relationship is dependent on the test piece configuration as noted by Ingelbrecht [9]. The maximum R-values achieved appeared to be independent of strain rate.

3.2. Mechanical properties

The proof and ultimate tensile strengths were slightly higher (15–19 MPa) in the L direction compared with the T direction after pressing the tube flat (Table I).

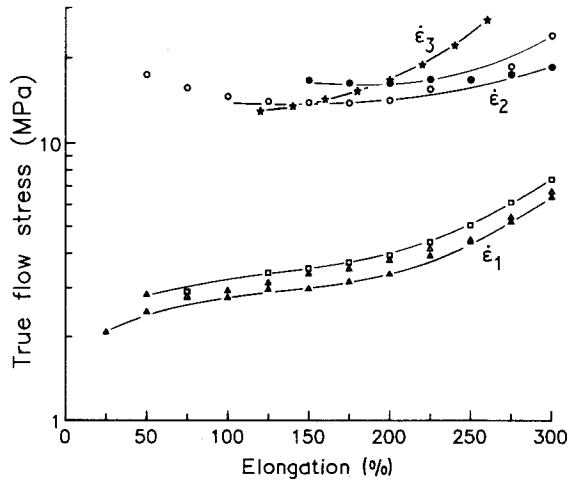

Figure 5 The continuous true flow stress versus percentage elongation at different strain rates, $\dot{\varepsilon}_1 = 5 \times 10^{-5}\ s^{-1}$, $\dot{\varepsilon}_2 = 3.2 \times 10^{-4}\ s^{-1}$, $\dot{\varepsilon}_3 = 1 \times 10^{-3}\ s^{-1}$. Test pieces: (●) L_1, (▲) L_2, (○) T_1, (△) T_2, (□) T_3, (★) T_5.

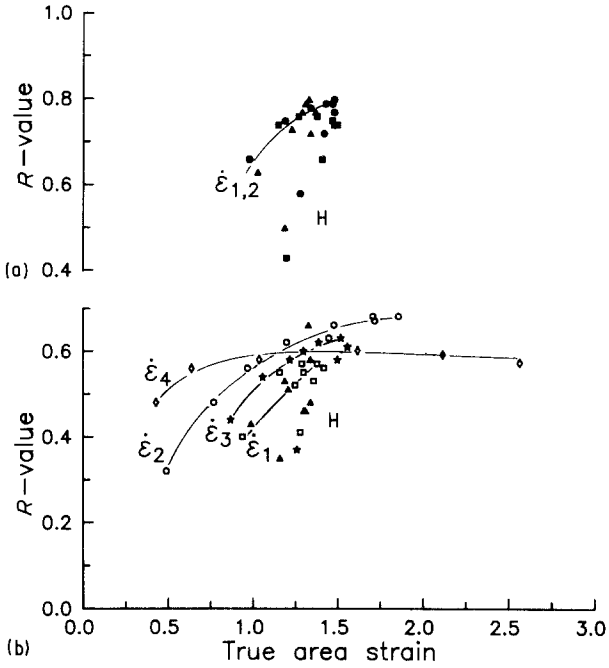

Figure 6 R-value versus true area strain after deformation at 925 °C and $\dot{\varepsilon}_1 = 5 \times 10^{-5}\ s^{-1}$, $\dot{\varepsilon}_2 = 3.2 \times 10^{-4}\ s^{-1}$, $\dot{\varepsilon}_3 = 1 \times 10^{-3}\ s^{-1}$, $\dot{\varepsilon}_4 = 1 \times 10^{-2}\ s^{-1}$ for (a) L test-pieces (●) L_1, (▲) L_2, (■) L_3; (b) T test-pieces (○) T_1, (△) T_2, (□) T_3, (★) T_4, (◇) T_5.

After the SPF thermal cycle (0% deformation, 925 °C for 7.5 h) the UTS was unchanged but the proof stresses decreased by 4.5%–10%. Compared with as-pressed material, the superplastic true strain of 1.4 reduced the proof stresses and the UTS by upto 8% (L-961 MPa, T-988 MPa) but the total elongation to failure was unchanged at 8%–12%. Young's modulus increased from 110 GPa (as-pressed) to 127 GPa after the thermal cycle. After superplastic deformation the modulus was ~ 110 GPa in the L test piece and ~ 125 GPa in the T test piece.

3.3. Microstructure

The microstructure of the extruded tube (Fig. 7) was not effected by pressing flat and showed equiaxed

TABLE I Tensile properties of Ti–6Al–4V extruded tube

Condition		Proof stresses (MPa)			Tensile strength (MPa)	Total elongation (%)	Young's modulus (GPa)
		0.1%	0.2%	0.5%			
As-pressed	L[b]	970	969	970	1045	11.3	110
	T[b]	944	949	953	1029	12.0	107
SPF thermal cycle[a]	L[b]	868	936	955	1042	17.0	127
	T[b]	903	936	942	1024	13.7	128
After SPF ($\varepsilon_{true} = 1.38$)	L[c]	838	855	885	961	8.0	112
	T[c]	877	893	911	988	12.3	125

[a]Thermal cycle, 925 °C for 7.5 h, slowly cooled (25 °C min^{-1} to 600 °C).
[b]Standard B-size test-piece.
[c]Machined from SPF test-piece.

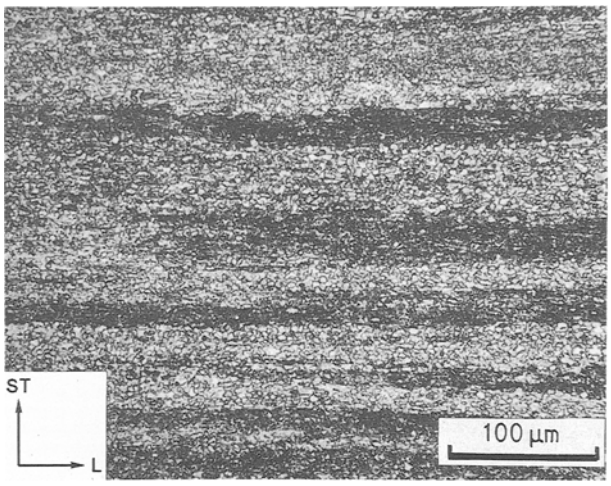

Figure 7 The banded microstructure in as-flattened material after heat treatment at 925 °C (5 min) and water-quenched.

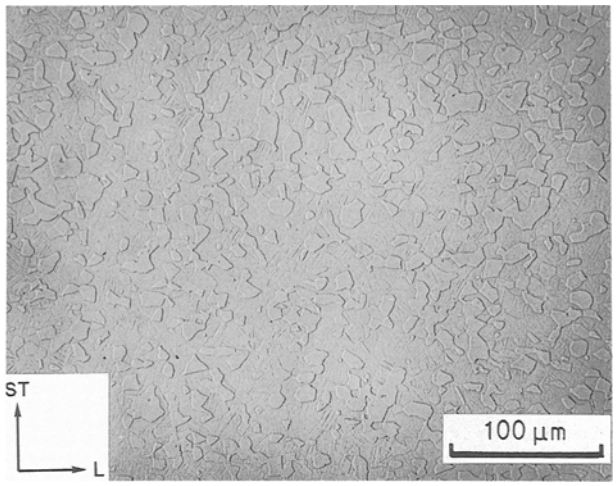

Figure 9 Equiaxed microstructure in a T test piece after superplastic deformation at 925 °C and $\dot{\varepsilon}_1$, $\varepsilon = 1.46$ and heat treatment at 925 °C (5 min) and water-quenched.

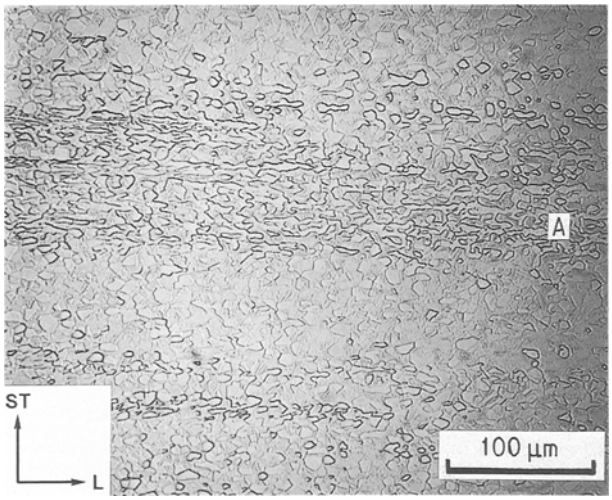

Figure 8 Contiguous α-phase band at A after the SPF thermal cycle and heat treatment at 925 °C (5 min) and water-quenched.

TABLE II The surface roughness of Ti–6Al–4V extruded tube after superplastic deformation ($\varepsilon = 1.38$, traverse length = 17.5 mm)

Test piece	R_a (μm)
Longitudinal (L_3)	1.76
Transverse (T_3)	9.08

grains of α and β phases with bands of contiguous α-phase orientated parallel to the extrusion (L) direction. The α-phase bands were most prominent in the ST–L plane, and here the α-phase had an aspect ratio of ~ 1.8; however between the contiguous α bands the α-phase was more equiaxed, with an aspect ratio of 1.1–1.3. The equiaxed α-grain size was about 4 μm.

After the SPF thermal cycle the α-grain size increased to ~ 7 μm and the contiguous α-bands remained in the ST–L plane (Fig. 8) with an aspect ratio similar to that of the as-pressed material. An α-phase grain size of 12–14 μm was determined after superplastic deformation at $\dot{\varepsilon}_1$, the contiguous α bands were no longer observed and the α-phase aspect ratio was 1.0 (Fig. 9). Surface ridges, perpendicular to the tensile axis were prominent on the T test pieces but much less apparent on the L test pieces (compare L3 and T3, Fig. 2). Consequently, much greater surface roughness was obtained for T test pieces than for L test pieces measured along the tensile axis after superplastic deformation (Table II). Careful sectioning through these surface ridges revealed residual α-phase bands at, or near the surface (Fig. 10). Talysurf measurements perpendicular to the tensile axis were not possible due to curvature in the test pieces.

In the α-phase texture of the as-flattened material the *c*-axis of the hcp α-phase was orientated parallel and at ~ 80° to the extrusion (L) direction and the

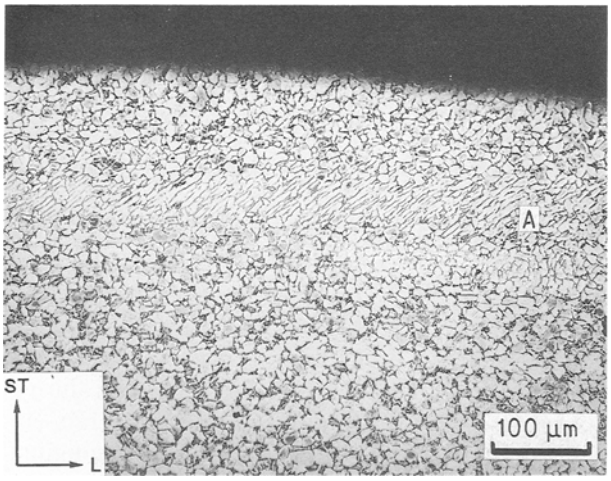

Figure 10 Residual contiguous α-phase at A associated with surface ridges on T test-pieces after superplastic deformation.

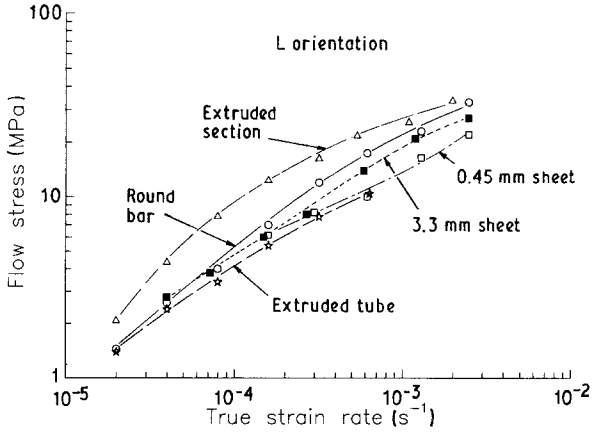

Figure 11 True flow stress versus true strain rate for sheet, bar and extruded Ti–6Al–4V products deformed at 925 °C.

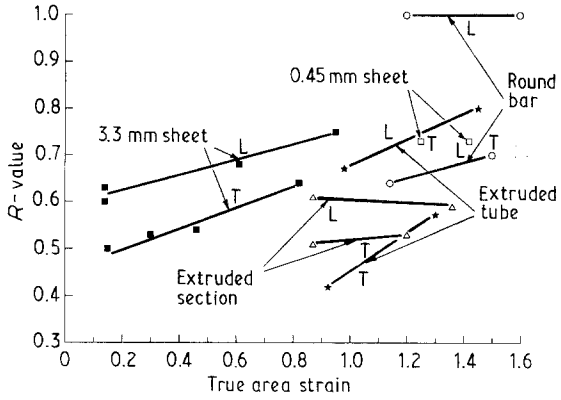

Figure 12 R value versus true strain after superplastic deformation at 925 °C for 0.45 and 3.3 mm thick sheet ($\dot{\varepsilon} = 3 \times 10^{-4}\ s^{-1}$), round bar ($\dot{\varepsilon} = 9 \times 10^{-5}\ s^{-1}$), extruded tube ($\dot{\varepsilon} = 5 \times 10^{-5}\ s^{-1}$) and extruded U section ($\dot{\varepsilon} = 2 \times 10^{-4}\ s^{-1}$).

texture was uniform through the thickness of the tube wall. Superplastic deformation at $\dot{\varepsilon}_1$ to 300 % of L test pieces had significantly randomized the α-phase texture but had little effect on T [8].

4. Discussion

Data were obtained in the present test programme on extruded Ti–6Al–4V alloy tube on the superplastic forming parameters, the isotropy of plastic flow and the post-formed mechanical properties. These data are essential for the successful exploitation of superplastic forming. Whilst superplastic forming parameter data are available for many materials, there is a dearth of data on the isotropy of plastic flow and the post-formed mechanical properties.

The present results show that the optimum strain rate for superplastic deformation of the extruded tube at 925 °C is $\dot{\varepsilon}_1$, because these conditions give rise to dimensional uniformity, low flow stresses, m-values > 0.5 and minimum strain anisotropy. This strain rate is significantly less than the strain rates ($\dot{\varepsilon}_2$ or higher) favoured by industry for SPF of sheet. However, at the typical sheet deformation rate, $\dot{\varepsilon}_2$, both the L and T extruded tube test pieces exhibited good dimensional uniformity (Fig. 2) and the flow stress of the extruded tube was very similar to that of sheet material (Fig. 11). The flow stresses of the extruded tube were consistently lower than round bar and extruded U-section product forms in both L and T orientations.

R-values were indicative of strain anisotropy during superplastic forming, with the extruded tube anisotropy greater in the T test pieces. In comparison with sheet, the R-values were similar for the L oriented extruded tube, but lower for the T extruded tube and both L and T extruded U-section (Fig. 12). Component-forming from the extruded tube is expected to result in most deformation occurring in the hoop (T) direction; greater strain anisotropy may be anticipated in comparison with sheet structure SPF. The strain anisotropy is caused by contiguous α-phase, aligned in the extrusion or rolling (L) direction which resists grain-boundary sliding and behaves as relatively undeformable stringers or islands surrounded by the softer β-phase (6, 10–12), this is particularly pronounced for the round bar (Fig. 12). In T test pieces the contiguous α-phase is aligned perpendicular to the tensile axis and limits the width strain [11, 13]. Because much of the strain takes place in the softer β phase this is also consistent with the lower flow stresses noted for the extruded tube T test pieces. In both T and L test pieces once the relatively easy shear paths along the β/β and α/β grain boundaries have been exhausted, shear will break up the contiguous α-phase to give the observed equiaxed microstructure associated with higher R-values [11]. Russian work has shown that a laminar microstructure in titanium alloy VT9 was converted to a near equiaxed microstructure after 70 % superplastic strain [14] but greater strains (200%) were required in Ti–6Al–4V rolled rectangular section bar [12]. Because there is greater constraint on the contiguous α-phase when it is oriented parallel to the tensile axis (L test pieces), it is more readily sheared and the microstructure becomes more rapidly equiaxed with increasing strain. Hence resistance to width strain is reduced and the anisotropy less for L test pieces than for T test pieces. An analogous situation exists in laser-welded joints in superplastically deformed Ti–6Al–4V sheet [15] in

which the constrained weld microstructure is converted to a more equiaxed microstructure in L test pieces. To avoid anisotropic superplastic deformation, a more homogeneous phase distribution is required and this may be possible via a thermo-mechanical preforming operation prior to extrusion.

Contiguous α-phase is also responsible for surface roughening of the extruded material during superplastic deformation, particularly in T test pieces where surface bands were noted. Roughening caused by residual bands of contiguous α-phase has been reported in rectangular section bars [16] and thin sheets [13]. In very thin (0.45 mm thick) Ti–6Al–4V sheet, surface roughening on a much finer scale occurred during superplastic strain and was caused by grain-boundary sliding [17]. In applications where contamination of a rough surface may be unacceptable, pickling after deformation may be required to reduce the surface roughness.

Texture does not effect deformation under superplastic conditions but changes in texture caused by superplastic deformation can affect the isotropy in post-formed mechanical tests at room temperature. Kaibyshev *et al.* [18] reported that crystallographic texture affected the high-temperature deformation behaviour of the titanium alloy VT6 (in the region of 700–900 °C) and of the Zn–22Al alloy [19], but the effect of texture decreased with increasing temperature. For Ti–6Al–4V, texture effects have been shown to be only significant at high strain rates ($\dot{\varepsilon} > 1 \times 10^{-2}\ s^{-1}$) or at temperatures below 800 °C corresponding to the transition from grain-boundary sliding to slip-controlled deformation [16].

The α-phase texture of L test pieces was randomized by superplastic deformation [8]; this may be explained by a grain-boundary sliding mechanism [12, 13, 20] which breaks up the contiguous α-phase and in this example causes significant grain rotation. The texture in T test pieces was essentially unchanged by superplastic deformation despite the change to a more uniform phase distribution after superplastic deformation, suggesting that much less grain rotation had occurred than in L test pieces. This was similar to the behaviour of extruded U-section [21] and rolled rectangular section bar [10], in which the texture was weakened but otherwise unchanged by similar superplastic strains. In two-phase Zn–Al alloy, unchanged texture was attributed to simultaneous slip deformation and grain-boundary sliding during superplastic deformation [22]. Despite the small change in the α-phase texture of T test pieces from the extruded tube, large changes in the β-phase texture of (both T and L orientations) are likely because most of the deformation is accommodated in this phase [10].

Although the *m*-values were relatively low compared to other Ti–6Al–4V product forms [23], good dimensional uniformity along the gauge length of test pieces was obtained up to strain rates of $\dot{\varepsilon} = 1 \times 10^{-3}\ s^{-1}$, this was probably related to the flat *m* versus $\dot{\varepsilon}$ curve for the extruded tube (Fig. 4). Work on Ti–6Al–4V rolled round bar [23] showed a steeply decreasing *m* versus $\dot{\varepsilon}$ curve ($m = 0.8$ at $\dot{\varepsilon} = 3 \times 10^{-5}\ s^{-1}$) and this gave good dimensional uniformity to a strain rate of only $\dot{\varepsilon} = 9 \times 10^{-5}\ s^{-1}$. The higher strain rate for the tube may be an important characteristic because it may permit forming at relatively high (and thus economic) strain rates.

The tensile strength of the tube material was essentially unaffected by the SPF thermal cycle, despite an increase from 4 μm to 7 μm in the α-phase grain size. However, following superplastic strain of 1.4, a decrease in tensile strength of up to 8 % (L test piece) and ~ 4 % (T test piece) was observed, in agreement with work on Ti–6Al–4V sheet [24] and round bar [25]. This decrease was probably associated with a significant increase in the grain size (to 12–14 μm) during superplastic deformation. Superplastic strain-enhanced grain growth has been noted in aluminium and titanium alloys by many workers [12, 26–28]. The pronounced randomizing of the L test piece texture may be responsible for the greater reduction in strength in the L orientation [6]. Reductions in strength are largely unavoidable with this non-heat-treatable alloy, but the titanium alloy IMI550, for example, can be re-heat-treated after superplastic deformation to recover fully the tensile properties [29].

5. Conclusions

Ti–6Al–4V extruded tube, with a non-ideal SPF microstructure exhibits low flow stresses, *m*-values in excess of 0.5 and good dimensional uniformity after deformation at strain rates up to $\dot{\varepsilon} = 1 \times 10^{-3}\ s^{-1}$. With these forming parameters superplastic deformation may be an attractive route for forming products from extruded tube.

There was no change in the ductility of Young's modulus after superplastic deformation, but the tensile strength decreased slightly (~ 8 %) due to concurrent grain growth during deformation. Superplastic deformation increased the surface roughness of the extruded tube.

Strain anisotropy was more pronounced in the T test piece and was attributed to aligned contiguous α-phase. Superplastic deformation reduced the contiguity and produced a more homogeneous phase distribution of equiaxed grains, suggesting that a preforming operation may be beneficial as part of the extrusion process to improve the microstructure.

Acknowledgements

The authors thank IMI Titanium Ltd for the supply of the material and R. I. Butt for the tensile testing. This paper is published by permission of the Controller, HMSO, holder of Crown Copyright.

References

1. W. CHENG and L. YING-SHE, in Proceedings of the Conference "Superplasticity and superplastic forming", Blaine, Washington, USA, 1–4 August 1988, edited by C. H. Hamilton and N. E. Paton (TMS, Warrendale PA, 1988) pp. 327–31.
2. S. YAMAZAKI, T. OKA, Y. MAE and M. KOBAYASHI, *ibid.*, pp. 407–11.
3. M. KOBAYASHI, M. MIYAGAWA, N. FURUSHIRO, K. MATSUI and Y. NAKAZAWA: in Proceedings of the

Conference "Superplasticity", Grenoble, France, 16–19 September 1985, edited by B. Baudelet and M. Suery (CNRS, Paris, 1985) pp. 12.1–12.15.
4. N. RIDLEY and C. HAMMOND, in Proceedings of the Conference "Superplasticity and superplastic forming", Blaine, Washington, USA, 1–4 August 1988, edited by C. H. Hamilton and N. E. Paton (TMS, Warrendale, 1988) pp. 365–76.
5. J. A. WERT and N. E. PATON, *Met. Trans.* **14A** (1983) 2535.
6. D. S. McDARMAID, A. W. BOWEN and P. G. PARTRIDGE, *J. Mater. Sci.* **19** (1984) 2378.
7. O. D. SHERBY and J. WADSWORTH, in "AGARD Lecture Series No. 168, Superplasticity" (NATO, Nevilly sur Seine, France, 1989) pp. 3.1–3.24.
8. A. WISBEY, P. G. PARTRIDGE and A. W. BOWEN, Technical Report 90060, Royal Aerospace Establishment, Farnborough, UK (1990).
9. C. D. INGELBRECHT, PhD thesis, University of Surrey, UK (1985).
10. A. W. BOWEN, D. S. McDARMAID and P. G. PARTRIDGE, *J. Mater. Sci.* **26** (1991) 3457.
11. P. G. PARTRIDGE, D. S. McDARMAID and A. W. BOWEN, *Acta Metall.* **33** (1985) 571.
12. D. S. McDARMAID, A. W. BOWEN and P. G. PARTRIDGE, *J. Mater. Sci.* **20** (1985) 1976.
13. C. D. INGELBRECHT and P. G. PARTRIDGE, *ibid.* **21** (1986) 4071.
14. O. A. KAIBYSHEV, in Proceedings of the Conference "Superplasticity and superplastic forming", Blaine, Washington, USA, 1–4 August 1988, edited by C. H. Hamilton and N. E. Paton (TMS, Warrendale, PA, 1988) pp 3–15.
15. P. G. PARTRIDGE, D. V. DUNFORD and S. PEACHEY, Technical Report 87066, Royal Aerospace Establishment, Farnborough, UK (1987).
16. D. S. McDARMAID and P. G. PARTRIDGE, *J. Mater. Sci.* **21** (1986) 1525.
17. P. G. PARTRIDGE, D. V. DUNFORD, in Proceedings of the Conference "Superplasticity and superplastic forming", Blaine, Washington, USA, 1–4 August 1988, edited by C. H. Hamilton and N. E. Paton (TMS, Warrendale, PA, 1988) pp. 215–20.
18. O. A. KAIBYSHEV, I. V. KAZACHKOV and R. M. GALEEV, *J. Mater. Sci.* **16** (1981) 2501.
19. O. A. KAIBYSHEV, I. V. KAZACHKOV and S. Ya. SALIKHOV, *Acta Metall.* **26** (1978) 1887.
20. R. H. BRICKNELL and J. W. EDINGTON, *Acta Metall.* **27** (1979) 1313.
21. A. W. BOWEN, D. V. DUNFORD and P. G. PARTRIDGE, in Proceedings of the Conference "Sixth World Conference on Titanium", Cannes, France, 1988, edited by P. Lacombe, A. Tricot and G. Béranger (Les editions de physique, Les Ulis Cedex, 1988) pp. 1367–72.
22. K. N. MELTON, J. W. EDINGTON, J. S. KALLEND and C. P. CUTLER, *Acta Metall.* **22** (1974) 165.
23. D. V. DUNFORD, A. WISBEY and P. G. PARTRIDGE, *Mater. Sci. Technol.* **7** (1991) 62.
24. C. D. INGELBRECHT, Technical Report 86015, Royal Aerospace Establishment, Farnborough, UK (1986)
25. D. V. DUNFORD and P. G. PARTRIDGE in Proceedings of the Conference "Superplasticity and superplastic forming", Blaine, Washington, USA, 1–4 August 1988, edited by C. H. Hamilton and N. E. Paton (TMS, Warrendale, PA, 1988) pp. 209–14.
26. D. S. McDARMAID, *Mater. Sci. Engng* **70** (1985) 123.
27. A. ARIELI, B. J. MACLEAN and A. K. MUKHERJEE, *Res. Mech.* **6** (1983) 131.
28. P. G. PARTRIDGE and A. J. SHAKESHEFF, *J. Mater. Sci.* **20** (1985) 2408.
29. C. D. INGELBRECHT, in Proceedings of the Conference "Designing with titanium", Bristol, UK, 1986, edited by P. H. Morton (Institute of Metals, London, 1986) p. 252.

Received 8 August
and accepted 10 September 1991